Acta Mech. Sin. (2015) 31(5):750–761
DOI 10.1007/s10409-015-0428-3

RESEARCH PAPER

Feasibility study on buoyancy–weight ratios of a submerged floating tunnel prototype subjected to hydrodynamic loads

Xu Long[1] · **Fei Ge**[2] · **Youshi Hong**[2]

Received: 8 December 2014 / Revised: 5 February 2015 / Accepted: 25 March 2015 / Published online: 16 July 2015

Abstract The research progress of a novel traffic solution, a submerged floating tunnel (SFT), is reviewed in terms of a study approach and loading scenario. Among existing publications, the buoyancy–weight ratio (BWR) is usually predefined. However, BWR is a critical structural parameter that tremendously affects the dynamic behaviour of not only the tunnel tube itself but also the cable system. In the context of a SFT prototype (SFTP) project in Qiandao Lake (Zhejiang Province, China), the importance of BWR is illustrated by finite element analysis and subsequently, an optimized BWR is proposed within a reasonable range in the present study. In the numerical model, structural damping is identified to be of importance. Rayleigh damping and the corresponding Rayleigh coefficients are attained through a sensitivity study, which shows that the adopted damping ratios are fairly suitable for SFTP. Lastly, the human sense of security is considered by quantifying the comfort index, which helps further optimize BWR in the SFTP structural parameter design.

Keywords Submerged floating tunnel · Buoyancy–weight ratio · Water wave and current loads · Dynamic response · Human security sense · Comfort index

✉ Xu Long
xulong@nwpu.edu.cn

[1] School of Mechanics, Civil Engineering and Architecture, Northwestern Polytechnical University, Xi'an 710072, China

[2] State Key Laboratory of Nonlinear Mechanics, Institute of Mechanics, Chinese Academy of Sciences, Beijing 100190, China

1 Introduction

The submerged floating tunnel (SFT), also named an Archimedes Bridge, is a novel kind of traffic solution for waterway crossings. In 1997, Norwegian engineers hoped to build the world's first SFT at the Hogsøord crossing [1], after which, the construction of a SFT has been taken into consideration in some strait crossing projects in the last twenty years; however, due to technological challenges and political issues, to date, there is no developed or developing SFT project in the world yet.

Compared with traditional bridges and tunnels, a SFT offers some promising advantages from both the structural characteristics and a social value's point of view [2,3]: (1) a SFT is submerged at a certain depth under the water's surface; therefore, water waves, currents and even tsunamsi will impact less on SFT. (2) The cost of a SFT is proportional to the length of the tunnel, while the construction cost of suspension bridge grows exponentially with increasing length. (3) In some water areas where it is inconvenient to set up traditional bridges due to waterway traffic, visual scenes or protected landscapes, a SFT will show unique environment-friendly applicability to minimize environmental impacts of man-made construction, and (4) a SFT owns a small road slope compared with the underground tunnel, which is more energy efficient and, therefore, causes less air pollution of traffic.

With so many attractive advantages, active researches have been carried out in the engineering and academic research communities around the world. As the first rigorous study, Alan Grant [4] first proposed a SFT solution for the Messina Strait Crossing in Italy in 1969. Later on, many projects have been carried out in terms of theoretical, numerical, and experimental studies, especially in the

following aspects: structural dynamic analysis of the tunnel tube, and optimization of the cable system under some specific water environment with consideration of hydrodynamic loads (waves and currents), seismic load, accident load, and temperature load.

Among the previous works, the tunnel and cable systems have been well studied experimentally and numerically. One example is Kunisu et al. [5]. They carried out an experimental study on a SFT's cable characteristics under wave conditions and summarized wave forces and dynamic behaviour of tunnels with the boundary element method and the Morison Equation. Another example is Venkatramana et al. [6]. They experimentally investigated the horizontal and the vertical components of a model dynamic response in unidirectional flows with consideration of the effects of flow velocity, fluid drag forces, and eddies on the dynamic responses. Also, Dong et al. [7] used a mixed method to investigate temperature-induced internal forces of a curved SFT supported by tension legs and concluded that radial forces resulting from temperature changes are larger than axial forces in the tunnel tube with consideration of axial stiffness of cables and flexural rigidity, curvature radius and central angle of SFT tunnels. In addition, Hui et al. [8] developed theoretical calculation models for SFT subjected to impact load and the shock wave caused by underwater explosions outside the tunnel [9] based on energy conservation and momentum conservation during impact. Concerning the effects of earthquake and parametric excitation, Su and Sun [10] presented a mathematical equation for vibration of SFT tethers. Also, Xiang and Chao [11] investigated vortex-induced vibrations in a SFT system and developed a theoretical model for coupled tube-cable vibration to evaluate the SFT structural dynamic response to water currents.

Due to the complexity of dynamic analysis in the time domain, finite element method is preferred in this paper as a more feasible and reliable approach, rather than the other advanced meshfree approaches such as element free Galerkin method (EFGM) [12] and smoothed particle hydrodynamics (SPH) method [13,14]. For this purpose, Paik et al. [15] developed a dynamic analysis program to analyze SFTs subjected to wave loading by modelling the tunnel with 3D beam elements based on the boundary element method and linear potential theory. The influence of depth on radiation damping, added-mass and maximum wave force was discussed. Also, Di Pilato et al. [16] proposed a procedure for nonlinear 3D dynamic analyses of SFT under seismic excitation by encompassing slender bars with anchor elements and developed an ad hoc finite element for efficiently modeling the elements. In addition, Shi et al. [17] accounted for material and geometrical nonlinearities, soil-structure interaction, and multiple-support seismic excitation by developing a 3D finite element analysis procedure.

In addition to the theoretical investigations, some in-situ studies of SFT have also been conducted. An SFT prototype (SFTP) project (100 m long) in Qiandao Lake (Zhejiang, China) was initiated by the Sino-Italian Joint Laboratory for Archimedes Bridge (SIJLAB) [18,19]. With the types of actions generally subjected to SFT, Mazzolani et al. [19] performed numerical analysis on the behavior of three kinds of cable system configurations under hydrodynamic loads and discussed the most performing one under seismic loads. Hong and Ge [18] summarized research advances on dynamical response and structural integrity of SFTP subjected to hydrodynamic load and accidental load in several aspects including theoretical analysis, modeling, calculation, and experimental investigation. As another in-situ study, the Reinertsen Olav Olsen Group [20] demonstrated the feasibility of the SFT constructions particularly for Sognefjorden (the largest fjord in Norway and the third longest in the world) and for similar fjord crossings in general. The designed SFT is capable of withstanding all functional and environmental loads with ample margins. Lidvard [2] showed the possibility of adopting SFT to cross these deep and wide fjords on the Western coast with fixed connections.

It is noteworthy that the buoyancy–weight ratio (BWR), defined by the ratio of Archimedes buoyancy due to the displaced water volume of the self-weight, is usually accounted for as a predefined structural parameter in previous numerical computations and model experiments. This means that starting from the design stage of a project, the nonlinear effect of BWR on the dynamic response of a SFT under environmental loads is neglected. As Mazzolani et al. [19] pointed out, BWR represents the first important key for the design of a SFT. According to the numerical study of Long et al. [21], BWR is of particular importance among the SFT structural parameters governing the geometric and material properties of tunnel and cable. With regard to a tunnel tube, BWR influences not only the geometrical design of the tube but also the material choice, stress strength safety design, and integral stiffness of the SFT, etc.

Obviously, with the requirement of structural safety, Archimedes buoyancy must be larger than the self-weight of the SFT, that is, BWR should be larger than unity, and the net buoyancy should be balanced by cable systems assembled between tunnel and foundations. Therefore, BWR determines cable tensions and, subsequently, influences obviously the dynamic behavior of cable systems under hydrodynamic loads, such as the distribution of lock-in regions and the vortex-induced vibration [22]. Considering the in-situ situation, installation, and operation load (traffic and, if any pedestrians) will change the value of BWR in a certain range. Hence, in the feasibility analysis concerning this kind of novel traffic structure, it is an urgent challenge to find such an appropriate BWR range to optimize the SFT balance between upwards and downwards actions under environmental loads.

For an underwater traffic construction, structural safety is a vital factor in SFT design. In the first international conference dedicated solely to the SFT tunnel in 1996, Hakkaart [1] particularly emphasized safety aspects of SFTs including the psychological issues, such as movements must be kept below the limits of human observation. Human senses of security and comfort depend on the horizontal and vertical accelerations and frequencies of dynamic vibration [23], there is; however, limited relevant published studies on SFT [20] in terms of SFT structural characteristics since this kind of study involves lots of considerations regarding structural and environmental factors.

In this paper, the SFTP project by SIJLAB is taken as the study context in terms of environmental conditions and tunnel and cable system designs. For simplicity, the total cross-section equivalence method is proposed and a finite element model is set up in the commercial software ANSYS. With focus laid on different BWRs, the dynamic responses of SFTs under hydrodynamic loads (wave and current) are analyzed, and the corresponding optimal range of BWRs is proposed. Lastly, the human sense of security and comfort are discussed to further optimize the range of BWRs.

2 Methodology of simplifications in modelling the SFTP model

A SFT is designed to be submerged at a certain depth under the water surface. Due to the difference of Archimedes buoyancy and tunnel tube self-weight, the net buoyancy is balanced by cable systems connected between the tunnel tube and the waterbed foundation. In general, SFT consists of four parts: (1) tunnel tube, which allows traffic and pedestrians to get through the water area and contains self-weight to stabilize the whole SFT system, (2) the cable system, which is designed to roughly meet the force equilibrium in the static water but also ensure the SFT stability under a hydrodynamic situation, (3) a waterbed foundation, which provides supports for the cable system, and (4) a tunnel-shore connection, which provides the constraints at the ends of the SFT [24].

The design length of a SFTP is 100 m and the tunnel tube is submerged 4.2 m under the still water surface. The tunnel-shore connection with stress relaxation and transversal constraints is applied at one end, while the other three translational degrees of freedom are constrained at the other end. The configuration of cable systems are schematically shown in Fig. 1, where the two ends of cable are connected to the tunnel and the foundation with spherical hinges, respectively. The cross-section of a SFTP tube is designed with consideration of corrosion resistance, collision protection, and tunnel weight balance, etc., as shown in Fig. 2.

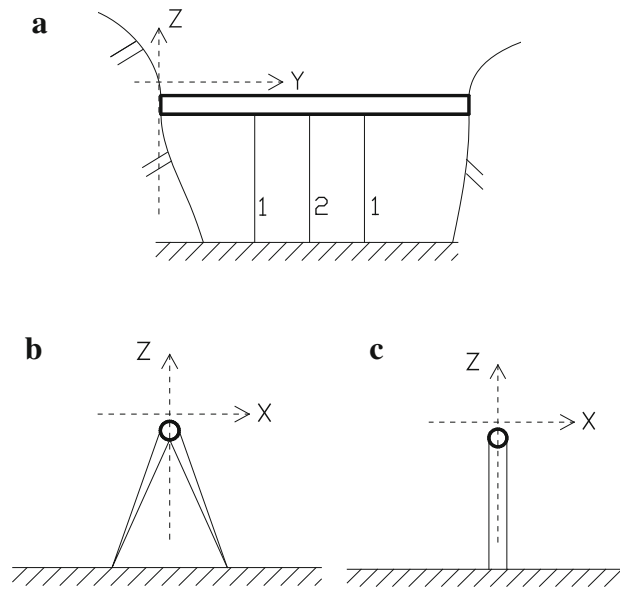

Fig. 1 Schematic diagram of SFTP. **a** Side elevation. **b** Cable system 1. **c** Cable system 2

2.1 Simplification of the tube cross-section

Based on the stiffness equivalent principle, the total cross-section equivalence method is proposed as

$$E_{\text{comp}} I_{\text{comp}} = E_{\text{Al}} I_{\text{Al}} + E_{\text{S}} I_{\text{S}} + E_{\text{C}} I_{\text{C}}, \tag{1}$$

$$I_{\text{comp}} = \frac{\pi}{64}(D^4 - d^4), \tag{2}$$

$$\rho_{\text{comp}} A_{\text{comp}} = \rho_{\text{A}} A_{\text{A}} + \rho_{\text{S}} A_{\text{S}} + \rho_{\text{C}} A_{\text{C}}, \tag{3}$$

where E, I, ρ, and A represent elastic modulus and cross-sectional moments of inertia, density, and cross-section area, respectively; the subscripts A, S, and C represent aluminum, steel, and concrete of the composite tube materials, respectively, while the subscript comp represents the simplified equivalent tube; D and d are the outer and inner diameters of SFTP tube.

With the same diameter of tunnel, the elastic modulus, and inner diameter of the equivalent SFTP tube can be obtained. The parameters of the simplified SFTP structure are listed in Table 1.

2.2 Calculation of hydrodynamic loads

The fluid environmental condition of Archimedes Bridge Bay where the SFT prototype is planned to be established is shown in Table 1. The Morison Equation expressed by Eq. (4) and Stokes fifth order wave theory are employed to obtain the fluid forces on the tube and the cables subjected to water waves and shear currents.

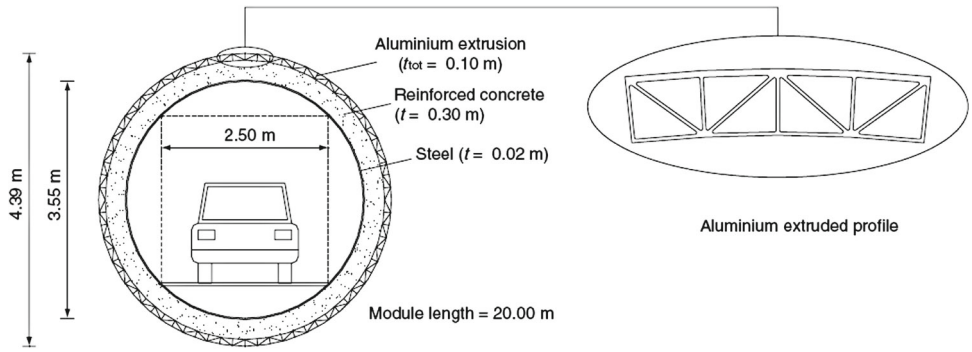

Fig. 2 Cross-section of the SFTP tube

Table 1 Parameters of SFTP structure and the fluid dynamic environment

Structural properties	Symbol	Unit	Value	Fluid dynamic environment	Symbol	Unit	Value
Tube equivalent density	ρ_T	kg/m^3	2018	Fluid density	ρ	kg/m^3	1050
Tube outer diameter	D	m	4.39	Water depth	h	m	30
Tube inner diameter	d	m	3.48	Wave height	H	m	1.0
Tube equivalent Young modulus	E_T	N/m^2	3.2×10^{10}	Wave period	T	s	1.8
Cable density	ρ_C	kg/m^3	7850	Surface current velocity	U_0	m/s	0.1
Cable diameter	d_C	m	0.06	Drag coefficient	C_D	1	1.0
Cable Young modulus	E_C	N/m^2	1.4×10^{11}	Mass coefficient	C_m	1	2.0
Kinetic viscosity Coefficient	υ	m^2/s	1.067×10^{-6}	Added-mass coefficient	C_a	1	1.0

$$f(t) = \frac{1}{2}C_D\rho D(u_w + u_c - \dot{x}_i)|u_w + u_c - \dot{x}_i| + C_m\rho\frac{\pi D^2}{4}\frac{\partial u_w}{\partial t} - C_a\rho\frac{\pi D^2}{4}\ddot{x}_i \quad (i = 1, 2), \tag{4}$$

where $x_i (i = 1, 2)$ is the displacement in X or Z direction; u_w and u_c are the fluid particle velocities on the axis of SFTP in X or Z direction; other parameters are defined in Table 1.

Undoubtedly, it is convenient to employ the Morison Equation proposed by Morison et al. [25] to calculate hydrodynamic loads, but the Morison Equation has its own scope of application $D/L < 0.2$, where D is the tunnel diameter while L is the wave length. As for deep water, L can be approximately equal to $gT^2/(2\pi)$, where g is the gravity acceleration. However, its scope of application is based on the assumption that the existence of an object does not break the motion of surface water waves. That is, this assumption is more suitable for the description of horizontal wave forces acting on a vertical pile extending from the bottom through the free surface [26]. For a SFT, with such a tube-type structure submerged transversely in some depth under the water surface, it is fairly reasonable to apply the Morison Equation to calculate the drag and inertia forces on SFT, even though the so-called scope of application has not been perfectly satisfied.

In order to stringently validate the application of the Morison Equation to a SFT, the predictions based on Morison Equation are investigated by comparing with those based on Stokes fifth order wave theory, which is usually adopted for floating and submerged structures. It is found that great agreement is achieved in the comparison and the discrepancy is negligible for the calculation of fluid forces on a SFT. In addition, the Morison Equation is a well-developed empirical formula and a vast library of drag force and inertia force coefficient data is available from numerous laboratories and field tests. Consequently, it is efficient to choose appropriate coefficients based on specific problems.

2.3 Structural damping

In the simplified numerical model of SFT, structural damping is considered in the form of a Rayleigh damping model, also known as a proportional damping model, to calculate the system damping matrix and preserve the simplicity of the real normal modes as in the cases without damping.

For a system with multi-degrees of freedom $\{X\}$ subjected to externally applied time-dependent force $\{P_t\}$, the equation of motion is given as

$$\boldsymbol{M}\{\ddot{X}\} + \boldsymbol{C}\{\dot{X}\} + \boldsymbol{K}\{X\} = \{P_t\}, \tag{5}$$

where $\boldsymbol{M}$, $\boldsymbol{C}$, and $\boldsymbol{K}$ are the mass, damping, and stiffness matrices.

Considering orthogonality property and assuming a diagonal damping matrix, Eq. (5) can be reduced to n uncoupled equations (see Eq. (6) where $j = 1, 2, \ldots, n$)

$$\{\ddot{\xi}\} + 2\zeta_j\omega_j\{\dot{\xi}\} + \omega_j^2\{\xi\} = \{P(t)\}. \tag{6}$$

According to the assumption of the Rayleigh damping model, the damping matrix $\boldsymbol{C}$ can be expressed as a linear combination of mass matrix $\boldsymbol{M}$ and stiffness matrix $\boldsymbol{K}$, as shown in Eq. (7)

$$\boldsymbol{C} = \alpha\boldsymbol{M} + \beta\boldsymbol{K}, \tag{7}$$

where the real scalars α and β are the Rayleigh damping coefficients. Then, Eq. (8) is obtained from Eq. (7) accordingly

$$\{\phi\}^{\mathrm{T}}\boldsymbol{C}\{\phi\} = \alpha\{\phi\}^{\mathrm{T}}\boldsymbol{M}\{\phi\} + \beta\{\phi\}^{\mathrm{T}}\boldsymbol{K}\{\phi\}, \tag{8}$$

where $\{\phi\}$ is the normalized eigenvector of the system. Comparing the damping matrices in Eqs. (6) and (8), Eq. (9) is achieved

$$[2\zeta_j\omega_j]_n = \begin{bmatrix} \alpha + \beta\omega_1^2 & 0 & . & . & 0 \\ 0 & \alpha + \beta\omega_2^2 & . & . & . \\ . & . & . & . & . \\ . & . & . & . & 0 \\ 0 & . & . & 0 & \alpha + \beta\omega_n^2 \end{bmatrix}. \tag{9}$$

From the symmetric characteristic, one can find that:

$$2\varsigma_j\omega_j = \alpha + \beta\omega_j^2 \quad \text{where} \quad j = 1, 2, \ldots, n. \tag{10}$$

If the damping ratios of two degrees of freedom (e.g., k-th and l-th) of the system could be well known, the Rayleigh damping coefficients α and β can be determined based on Eq. (11), which is further simplified from Eq. (10)

$$2\varsigma_k\omega_k = \alpha + \beta\omega_k^2, \qquad 2\varsigma_l\omega_l = \alpha + \beta\omega_l^2. \tag{11}$$

Nevertheless, for systems with a great number of degrees of freedom, in the beginning of the analysis it does not make sense to predefine the Rayleigh damping coefficients α and β. Thus, a procedure proposed by Chowdhury et al [27]. is capable of ensuring a rational estimate of these coefficients, which is assumed to be applicable to all of modes of vibration [27].

Different interpolations are adopted to find the best-fit regarding the rational values of α and β with different first m order choices in Eq. (12)

$$\zeta_i = \frac{\zeta_{\mathrm{m}} - \zeta_1}{\omega_{\mathrm{m}} - \omega_1}(\omega_i - \omega_1) + \zeta_1, \tag{12}$$

where ω_i and ς_i are the natural frequency and damping ratio for the i-th mode in the structural analysis, respectively. From the modal analysis of the SFTP computational model when BWR is 1.4, the results of the first 25 modes are obtained as listed in Table 2.

Referring to the numerical analysis of pipelines in the offshore industry, the damping ratio of the 1st vibration mode of SFTP is taken as 2.5 % as per Section 6.2.11 of the Recommended Practice DNV-RP-F105 [28]. The value has been compensated by considering the internal friction forces of material and the sliding between composite tube materials during deformation. On the other hand, the damping ratio of a higher vibration mode of interest is taken as a sufficiently

Table 2 Modal analysis of the SFTP model

No. of mode	Natural frequency (Hz)	Mass fraction	No. of mode	Natural frequency (Hz)	Mass fraction
1	0.814922	0.667382	14	18.442	0.964165
2	1.44753	0.667715	15	24.082	0.977084
3	2.31223	0.816431	16	24.094	0.977116
4	2.59909	0.816431	17	28.7504	0.977116
5	5.12123	0.883872	18	30.15	0.98631
6	5.17988	0.884035	19	30.1716	0.98631
7	8.79712	0.921598	20	30.4621	0.986311
8	8.82534	0.921598	21	36.5437	0.99416
9	10.1514	0.9216	22	36.565	0.994162
10	13.2933	0.947741	23	43.1625	0.994162
11	13.3655	0.947748	24	43.2187	0.999999
12	14.3678	0.947748	25	43.2213	1.00000

The cable is meshed with a single element to capture the tunnel vibration modes in the modal analysis and; therefore, the natural frequencies are conservatively different from those obtained later in the dynamic analysis with much finer meshes in cables

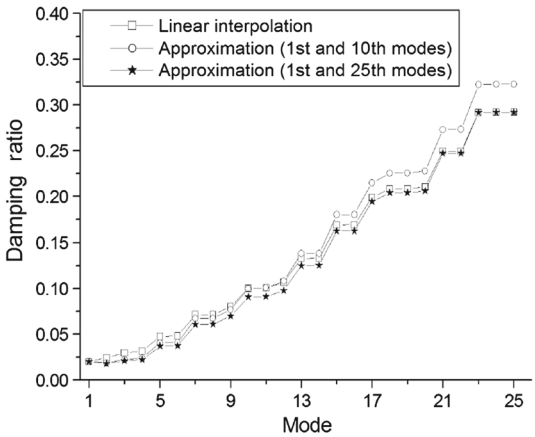

Fig. 3 Comparison of damping ratio with different interpolation methods

large value, e.g. 10 % in the present study. With the assumed damping ratios for the 1st and 10th vibration modes, the obtained damping ratios based on Eq. (12) and Eqs. (10) and (11) are indicated as "Linear interpolation" and "Approximation (1st and 10th modes)" in Fig. 3, respectively. In order to rule out the sensitivity regarding the choice of a higher vibration mode in Eqs. (10) and (11), the damping ratios are calculated again based on the 1st and 25th vibration modes and indicated as "Approximation (1st and 25th modes)" in Fig. 3.

Obviously, in Fig. 3, Rayleigh damping ratios from the first 10 and 25 vibration modes, respectively, are slightly less than those obtained from the linear interpolation method. However, it should be noted that in the first several vibration modes, the damping ratios are almost the same and do not vary with the increase of modes. On the other hand, as only the first few vibration modes are usually excited under the environmental loads, and, in addition, the mass fraction is concentrated at the first few vibration modes, as shown in Table 2, the effective vibration modes would be the first several ones. Thus, it is reasonable to use the same damping ratio (2.5 %) and the first two natural frequencies when conducting dynamic analysis for SFTP.

It is also noteworthy that the Rayleigh damping ratios based on different vibration modes (10th and 25th modes for the analysis shown in Fig. 3) are reasonably close; therefore, it is safely concluded that the Rayleigh damping coefficients in the first few vibration modes are not significantly sensitive to the frequency choice of vibration mode.

3 Numerical study of SFT

A numerical model is created by means of the commercial finite element analysis software ANSYS and the element PIPE59, from which the hydrodynamic loads can be developed based on the Morison Equation, is employed to discretize the SFT tunnel and cables, as shown in Fig. 4.

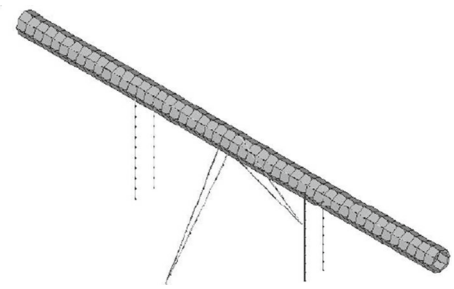

Fig. 4 FE computation model of SFTP

The geometric and material properties, hydrodynamic loads, and Rayleigh damping coefficients are incorporated into the finite element model according to the SFTP simplification methodology proposed in Sect. 2.

Particularly, the coefficients are calculated based on the damping ratio 2.5 % and the first two natural frequencies. For example, in the case when the BWR is 1.4, natural frequencies are 0.815 and 1.448 Hz, as given in Table 2, while damping coefficients α and β are respectively obtained as 0.586 and 0.00352 from Eqs. (10) and (11).

3.1 Dynamic analysis of SFTP without structural damping

With the simulations of SFTP under the hydrodynamic loads of Qiandao Lake, SFTPs in the BWR range between 1.1 and 1.9 are calculated in both the cases without and with structural damping. The dynamic responses at the mid-span of the SFTP tunnel and cable in the time history without consideration of structural damping are shown in Figs. 5 and 6. These tunnel and cable results indicate that in the current direction the tunnel vibration amplitude increases with increasing BWR from 1.1 to 1.9, which agrees well with the experimental conclusion regarding the specific gravity tunnel range between 0.51and 0.76 (that is BWR ranges between 1.32 and 1.96) under similar environmental loads and mooring systems as proposed by Susumu et al. [29].

Compared with the effect of BWR in the current direction, the amplitude in the vertical direction is more obviously influenced by BWR. More importantly, in the adjacent region with the BWR value of 1.2, the tunnel vibration amplitude arrives at a minimum value. This phenomenon can be simply verified by the theoretical conclusions of Clough and Penzien [30] that the vibration system having no damping under forced excitation will have a deleterious effect if the support system is too stiff.

As a structural parameter, BWR is more efficient in optimizing the vertical vibration stability than the horizontal vibration stability. In the practical engineering construction, more mitigation measures should be considered to deal with the horizontal dynamic response, such as adopting more effi-

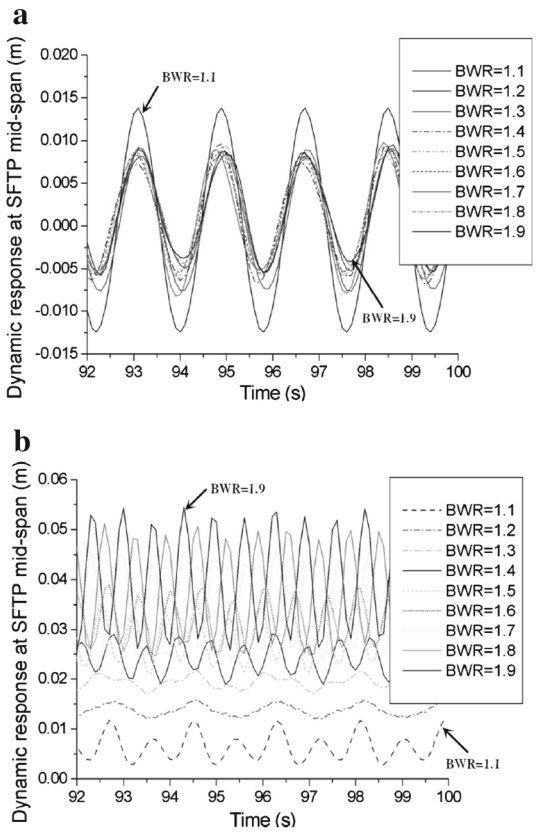

Fig. 5 Dynamic response at the mid-span of the SFTP tunnel without damping. **a** Current direction. **b** Vertical direction

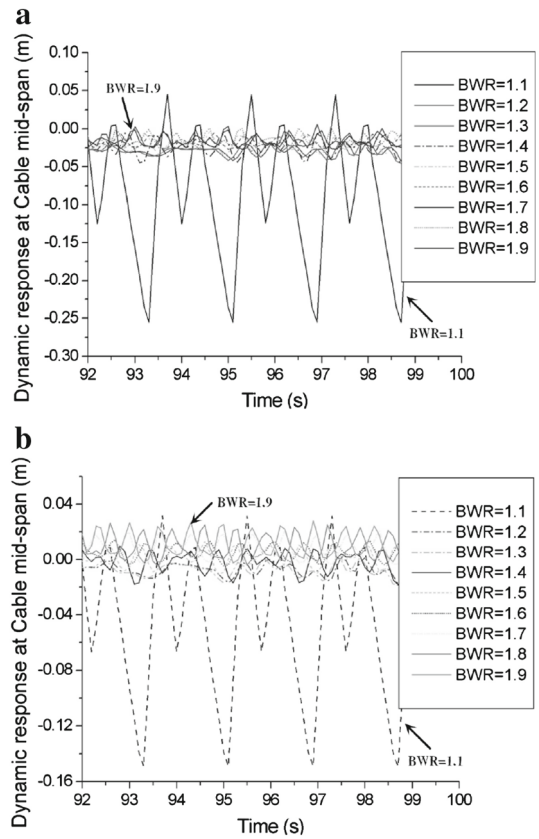

Fig. 6 Dynamic response at the mid-span of the SFTP cable system 2 without damping. **a** Current direction. **b** Vertical direction

cient horizontal constraints in the cable systems, settling up inertial dampers, and improving the toughness characteristic of the tunnel outer surface, etc.

As shown in Fig. 6, the influence of BWR on the cable dynamic response is straightforward. The amplitude of cable response in both current and vertical directions decreases as BWR increases. Notably, when BWR is larger than 1.2 the amplitude decreases marginally and almost keeps certain smaller value compared with that when BWR stays at 1.1.

3.2 The effect of structural damping on dynamic analysis of a SFTP

In order to rationally quantify the effect of structural damping when investigating the changing pattern of a SFT response with BWR, dynamic responses at the mid-span of the SFTP tunnel and cable in the same time history but with consideration of structural damping, are shown in Figs. 7 and 8, respectively.

The results in Figs. 7a and 8 show similar changing patterns with BWR in the current direction of SFTP and in both the current and vertical directions of the cables. But according to the dynamic response in the vertical direction of SFTP tunnel (see Fig. 7b), the vibration amplitude decreases steeply and then stays at a more stable value when BWR is equal to and greater than 1.2, as compared with the case without considering structural damping shown in Fig. 5b. With the aid of standard deviation (STDEV), dynamic responses at the mid-span of SFTP tunnel in the time history without consideration of structural damping is shown in detail in Fig. 9, where the ordinate is the standard deviation ratio of the dynamic response in a certain direction to the tunnel diameter (D), while the abscissa is BWR. Similarly, dynamic responses at the mid-span of SFTP tunnel in the time history with consideration of structural damping are shown in Fig. 10.

The changing pattern with BWR in Fig. 9b is significantly distinguished from that in Fig. 10b, and the obvious reason for this difference is the existence of structural damping brought into the computation model in the form of Rayleigh damping. These computation results for the cases with structural damping have been verified from a general trend point of view by a simple in-house experimental study [31]. Similar changing patterns of SFT dynamic response with different BWRs were observed and the same optimized BWR could be obtained, even though the absolute dynamic responses did not agree well. The discrepancy stemmed from some differences between the scaled-down experimental specimen and the full-scale SFT. The most influential assumption made

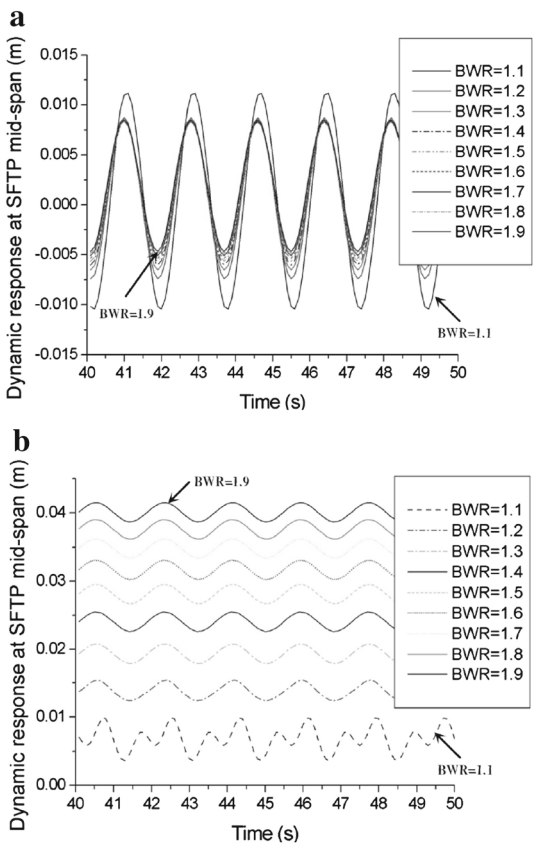

Fig. 7 Dynamic response at the mid-span of the SFTP tunnel with damping. **a** Current direction. **b** Vertical direction

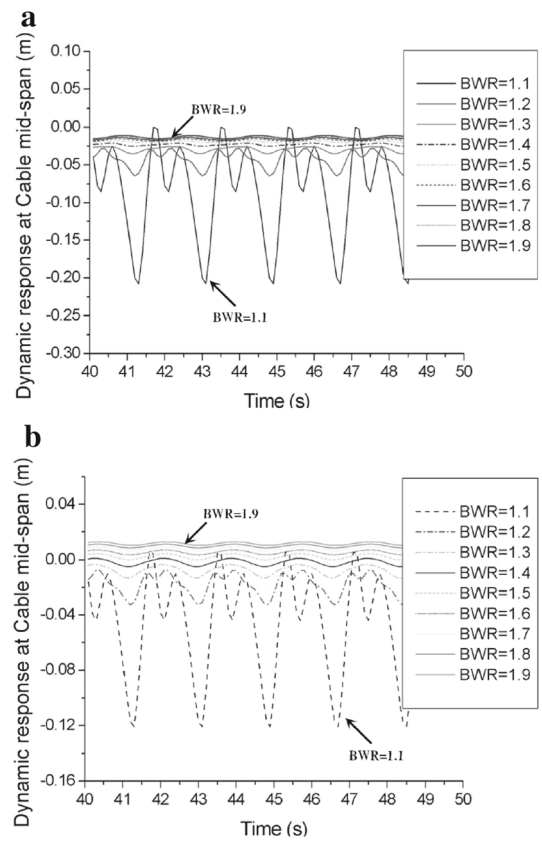

Fig. 8 Dynamic response at the mid-span of the SFTP cable system 2 with damping. **a** Current direction. **b** Vertical direction

is that with stiffness equivalence, linear-tensile springs with finite deformation capacity were used to simulate the cable supports with catenary action. In fact, a large displacement may occur and geometric nonlinearity cannot be simulated. On the other hand, due to the limit of the water tank, only the first wave attacking SFT was considered for comparison to rule out the effect of wave reflection. This may induce a highly unstable dynamic response, which is difficult to simulate in explicit finite element analysis. Thus, the model test was only a target to demonstrate the effect of BWR on SFT dynamic response. Definitely, this experimental approach is worth further in-depth study in the context of more reasonable simplifications and advanced laboratory instrumentations.

During the structural modal analysis of natural frequencies and Rayleigh coefficients, it is also noted that the damping coefficient α increases while β decreases as BWR increases from 1.1 to 1.9. In the damping matrix (see Eq. (7)), α and β are the weight coefficients for mass matrix and stiffness matrix, respectively. Thus, under the circumstance of such an SFTP, the influence of the mass matrix on structural damp increases, while the influence of the stiffness matrix on structural damp decreases. This phenomenon results in greater importance of structural damping in the SFT analysis to which more attention should be paid.

4 Human sense of security and comfort index

The sense of human security depends on the vibration acceleration and frequency. The sensitive frequency range is 1–2 Hz for the horizontal direction and 4–8 Hz for the vertical direction, while the threshold value of acceleration that a human can feel is $10^{-3}\,\mathrm{m/s^2}$ in the vertical direction and the ceiling value that a normal human can stand is $0.5\,\mathrm{m/s^2}$. Besides, the comfort index is also an issue of importance for ground vehicles and bridge engineering. In this study, the Sperling comfort index [32], based on acceleration amplitude and frequencies of vibration components identified by fast Fourier transform (FFT), is employed to assess the SFTP comfort under the hydrodynamic loads. Therefore, appropriately controlling vibration accelerations and frequencies of a SFTP tunnel will benefit people's feeling have and being comfortable.

The acceleration response of the SFTP tunnel under the amplitude-steady vibration is calculated. By means of the FFT method, power spectrum analysis is carried out based

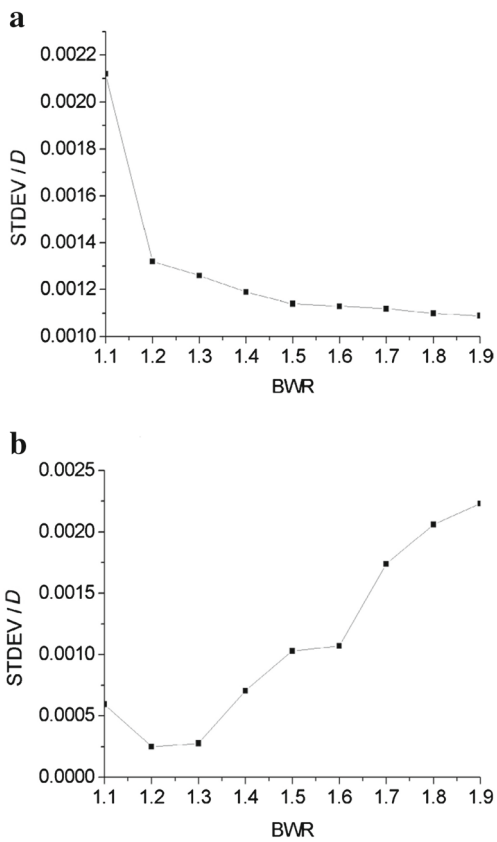

Fig. 9 Dynamic response at the mid-span of the tunnel without structural damping. **a** Current direction. **b** Vertical direction

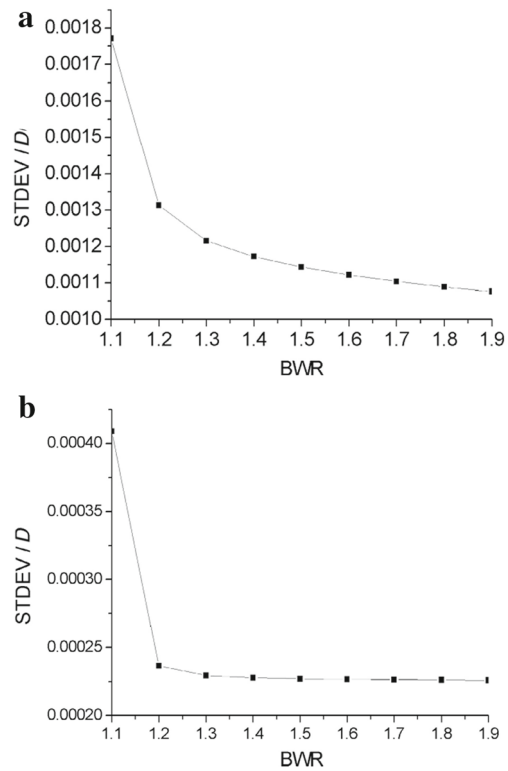

Fig. 10 Dynamic response at the mid-span of the tunnel with structural damping. **a** Current direction. **b** Vertical direction

on dynamic responses of SFTP models with different BWRs under water wave and current loads. After filtering signal noises, the dynamic response of the vibration component with a specific frequency in the time history can be obtained. For instance, excited frequencies of SFTP with BWR 1.1 and dynamic responses of the vibration components by filtering the wave signals of its vibration frequencies are shown in Fig. 11. Thus, based on the dynamic analysis results of SFTP for different BWRs, the amplitudes of acceleration responses of all different frequencies are obtained (see Table 3).

In Table 3, 0.55 Hz is the forced vibration frequency of wave load, while other frequencies are the natural frequencies excited by wave and current loads and the proportions of their energy in the whole vibration are much less. The changing pattern of vibration accelerations and frequencies in Table 3 indicates that the capability of BWR of SFTP to regulate the acceleration amplitude and frequencies in the vertical direction is not so remarkable. However, the vertical acceleration amplitude at the SFTP mid-span will stay at a steady and smaller value when BWR is larger than 1.1, which basically satisfies the human sense of security for a traffic environment where people can feel clearly but can tolerate the SFTP vibration.

At the same time, the dominating frequency of the tunnel in the current direction is 0.5469 Hz, which is also the forced vibration frequency of wave and current loads and is fortunately beyond the human sensitive range of 1–2 Hz. In the vertical direction when BWR is larger than 1.1, the contribution for structural acceleration response is from the vibration component with the frequency 1.25 Hz, which is also beyond the vertical sensitive range of 4–8 Hz. Therefore, tunnel vibration frequency does not harm the human sense of security for SFTP environments and the problem is located in the control of vertical acceleration responses.

With the changing pattern shown in Table 3, when BWR is equal to and larger than 1.2, the tunnel acceleration response in the current direction increases with the increase of BWR, while the tunnel acceleration response in the vertical direction increases extremely slowly and stays at a steady value of 0.02 m/s^2. Thus, in practical design and construction, BWR should be around 1.2 in order to reduce the acceleration amplitude both in the current and in the vertical directions as much as the design scheme can achieve.

Furthermore, in order to ensure the SFTP comfort for human beings, the Sperling comfort index (see Table 4) is referred to as the comfort standard of SFTP under hydrodynamic loads.

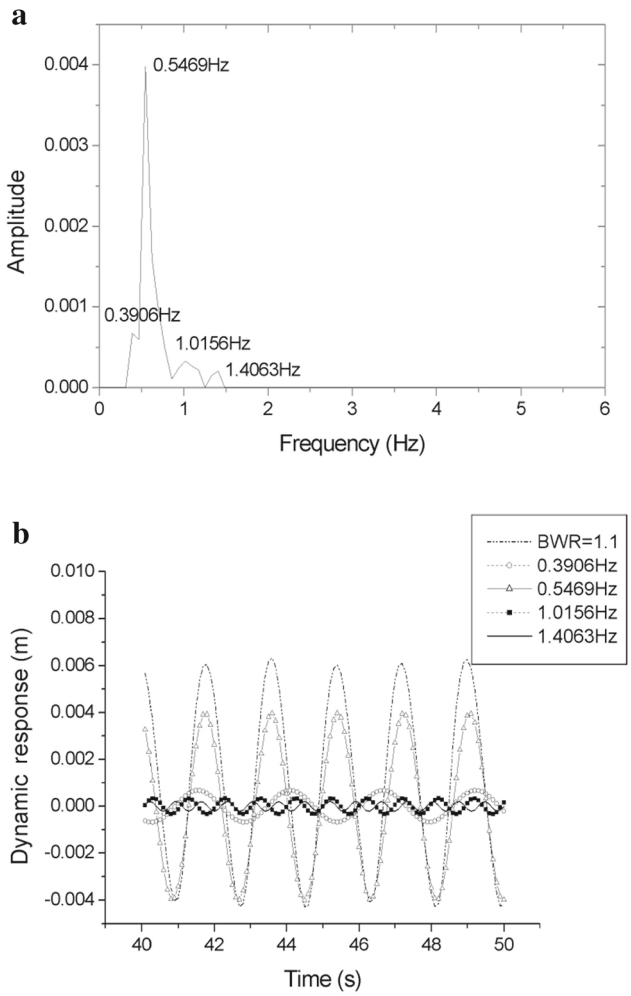

Fig. 11 Frequency and power spectrum analysis regarding SFTP. **a** Excited frequencies of SFTP. **b** Dynamic responses of vibration components

Table 4 Sperling comfort index

W_z	Comfort level
1.00	Just noticeable
2.00	Clearly noticeable
2.50	More pronounced but not unpleasant
3.00	Strong, irregular, but still tolerable

The Sperling comfort index is defined in Eq. (13).

$$W_z = \left(\sum_{i=1}^{n_f} W_{z_i}^{10} \right)^{\frac{1}{10}}, \tag{13}$$

where n_f is the total number of the discrete frequencies of the acceleration response identified by FFT, and W_{zi} is the comfort index corresponding to the i-th discrete frequency, computed as

$$W_{z_i} = [a_i^3 B(f_i)^3]^{\frac{1}{10}}, \tag{14}$$

where a_i denotes the amplitude of the acceleration response of the i-th frequency identified by FFT and $B(f_i)$ a weighting factor (see Eq. (15))

$$B(f_i) = 0.588 \times \left[\frac{1.911 f_i^2 + (0.25 f_i^2)^2}{(1 - 0.277 f_i^2)^2 + (1.563 f_i - 0.0368 f_i^3)^2} \right]^{\frac{1}{2}}. \tag{15}$$

By means of FFT and inverse transformation of FFT, dynamic responses of vibration component corresponding to every vibration frequency in the time history are adopted to assess

Table 3 Acceleration responses in time history and excited dominating frequencies of SFTP for different BWRs under water wave and current loads

BWR	Acceleration (m/s^2)		Frequency (Hz)	
	X	Z	X	Z
1.1	0.04562	0.03063	0.5469/1.1056/1.4063	0.5469/0.8594/1.1719
1.2	0.06195	0.02191	0.5469/1.1056/1.4063	0.5469/0.8594/1.2500
1.3	0.07060	0.02047	0.5469/1.1056/1.4063	0.5469/0.8594/1.2500
1.4	0.07537	0.02029	0.5469/1.1056/1.4063	0.5469/0.8594/1.2500
1.5	0.08123	0.02020	0.5469/1.1056/1.4063	0.5469/0.8594/1.2500
1.6	0.08769	0.02001	0.5469/1.1056/1.4063	0.5469/0.8594/1.2500
1.7	0.09225	0.01999	0.5469/1.1056/1.4063	0.5469/0.8594/1.2500
1.8	0.09565	0.01995	0.5469/1.1056/1.4063	0.5469/0.8594/1.2500
1.9	0.09976	0.01998	0.5469/1.1056/1.4063	0.5469/0.8594/1.2500

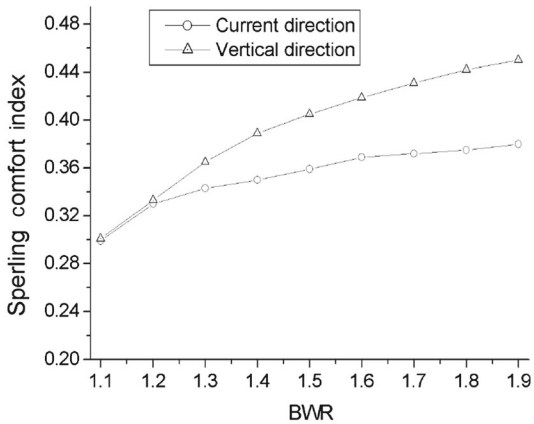

Fig. 12 Sperling comfort index at the mid-span of a SFTP with different BWRs

the Sperling comfort index as the reference of SFTP comfort for human beings. The Sperling comfort indexes both in the current and in the vertical directions are shown in Fig. 12.

Figure 12 indicates that compared with the vertical direction result, BWR influences the Sperling comfort index more weakly. In the BWR range between 1.1 and 1.2, the comfort indexes in both the current and the vertical directions are optimized. On the whole, due to the mild fluid dynamic environment of SFTP, dynamic responses of SFTP under water wave and current loads have little influence on the human comfort index which lies in the range of "just noticeable".

Considering the SFTP structural safety, BWR must be larger than 1.0. When BWR is too small, SFTP keeps freely submerged under the still water surface, and there is no displacement constraint to ensure the tunnel location. What is more, combining the conclusions from the human sense of security and the Sperling comfort index based on the analysis of SFTP vibration accelerations and frequencies, the suggestion is that the BWR is to be around 1.2 in the practical structural parameter design.

Regarding human comfort, evacuation measures should be taken into account once there is an emergency. Some researchers have proposed the philosophy of emergency escape devices [33] and investigated the effect of these devices on the hydrodynamic load acting on a SFT in uniform and oscillatory flows and water waves by numerical tests [34]. However, besides the safety issue, the psychological influence on people should also be further studied and addressed as there is such a confined space inside the tunnel.

5 Conclusion and discussion

As the most fundamental structural parameter, BWR should be optimized in the first place before performing the other detailed engineering designs. In this paper, a preliminary numerical study is carried out to determine the optimal value of BWR in the context of a SFTP project. Several general conclusions are drawn as follows.

(1) Changing patterns of dynamic responses of SFTPs with increasing BWRs under water waves and current loads indicate the opportunity and efficiency of adopting certain BWRs to optimize the dynamic behavior of a SFTP tunnel and cable. For this study in Qiandao Lake, a BWR of 1.2 could be the most promising choice in the SFTP structural parameter design.
(2) Considering the structural damping in the computation model, different changing patterns of dynamic responses of SFTPs with increasing BWRs under water waves and current loads are shown, which results from the change of the Rayleigh coefficient in the case considering the structural damping, specifically, the weighting factors of the mass matrix and the stiffness matrix change with the increase of BWRs in the calculation of damping matrix.
(3) What should be noted is that whether structural damping is considered or not, an obvious alternation of changing patterns of SFTP tunnel dynamic responses with the increase of BWRs will happen in the adjacent region where BWR equals 1.2.
(4) Under water waves and current loads, dynamic responses of a SFTP tunnel with a BWR located around 1.2 in both the current and the vertical directions basically satisfy, in regard of vibration acceleration and frequencies, the requirement of human senses of security and comfort.

It should be noted that the proposed range of BWR is only based on the preliminary structural study at the design and construction stages. Nevertheless, the proposed methodology based on finite element simulations is applicable to a SFT under any loading scenarios, even though the optimized BWR can vary due to the additional loads induced at the stages of installation and operation [35,36]. If the applied loads are unexpected, some technical measures [37] should be taken at the operation stage to adjust the SFT buoyancy and maintain a reasonably optimized dynamic response. On the other hand, the methodology proposed is to conduct the optimization of BWR in the hydrodynamic conditions at Qiandao Lake, rather than providing a universal BWR range for all the SFTs of interest. In addition, more studies should be conducted later on for analysis concerning local buckling, free spanning, fatigue, strain concentration, and fracture.

References

1. Ahrens, D.: Submerged floating tunnels—a concept whose time has arrived. Tunn. Undergr. Space Technol. **12**, 317–336 (1997)

2. Lidvard, S.: Crossing the deep and wide fjords on the western coast of Norway with fixed connections. In: Proceedings of the 6th International Conference. Bergen, Norway (2013)
3. Tveit, P.: Ideas on downward arched and other underwater concrete tunnels. Tunn. Undergr. Space Technol. **15**, 69–78 (2013)
4. Faggiano, B., Landolfo, R., Mazzolani, F.: Design and modelling aspects concerning the submerged floating tunnels: An application to the Messina Strait crossing. In: Proceedings of the 3rd International Conference on Strait Crossings. Bergen, Norway (2000)
5. Kunisu, H., Mizuno, S., Mizuno, Y., et al.: Study on submerged floating tunnel characteristics under the wave condition. The Fourth International Offshore and Polar Engineering Conference: International Society of Offshore and Polar Engineers (ISOPE), 27–32 (1994)
6. Venkataramana, K., Yoshihara, S., Toyoda, S., et al.: Current-induced vibrations of submerged floating tunnels. The Sixth International Offshore and Polar Engineering Conference. Los Angeles, USA: International Society of Offshore and Polar Engineers (ISOPE), 111–118 (1996)
7. Dong, M.S., Ge, F., Hong, Y.S.: Analysis of thermal internal forces for curved submerged floating tunnel. Eng. Mech. **23**, 2l–24 (2006)
8. Hui, L., Ge, F., Hong, Y.S.: Calculation model and numerical simulation of submerged floating tunnel subjected to impact loading. Eng. Mech. **2**, 038 (2008)
9. Hui, L.: Dynamic response of submerged floating tunnel under accident loading, [MS Dissertation]. Institute of Mechanics, Graduate University of Chinese Academy of Sciences, Beijing, China (2007) (in Chinese)
10. Su, Z.B., Sun, S.N.: Seismic response of submerged floating tunnel tether. China Ocean Eng. **27**, 43–50 (2013)
11. Xiang, Y.Q., Chao, C.F.: Vortex-induced dynamic response analysis for the submerged floating tunnel system under the effect of currents. J Waterw Port Coast Ocean Eng-ASCE **139**, 183–189 (2013)
12. Yin, Y., Yao, L.Q., Cao, Y.: A 3D shell-like approach using element-free Galerkin method for analysis of thin and thick plate structures. Acta Mech. Sin. **29**, 85–98 (2013)
13. Ming, F.R., Zhang, A.M., Cao, X.Y.: A robust shell element in meshfree SPH method. Acta Mech. Sin. **29**, 241–255 (2013)
14. Han, Y.W., Qiang, H.F., Liu, H., et al.: An enhanced treatment of boundary conditions in implicit smoothed particle hydrodynamics. Acta Mech. Sin. **30**, 37–49 (2014)
15. Paik, I.Y., Oh, C.K., Kwon, J.S., et al.: Analysis of wave force induced dynamic response of submerged floating tunnel. KSCE J. Civ. Eng. **8**, 543–550 (2004)
16. Di Pilato, M., Perotti, F., Fogazzi, P.: 3D dynamic response of submerged floating tunnels under seismic and hydrodynamic excitation. Eng. Struct. **30**, 268–281 (2008)
17. Shi, C.X., Domaneschi, M., Martinelli, L.: Nonlinear behaviors of submerged floating tunnels under seismic excitation. In: Zhang, C., Lin, P.P. (eds.) Vibration, Structural Engineering and Measurement Ii, Pts 1–3, 1124–1127. Trans Tech Publications Ltd, Stafa-Zurich (2012)
18. Hong, Y.S., Ge, F.: Dynamic response and structural integrity of submerged floating tunnel due to hydrodynamic load and accidental load. Procedia Eng. **4**, 35–50 (2010)
19. Mazzolani, F.M., Landolfo, R., Faggiano, B., et al.: Structural analyses of the submerged floating tunnel prototype in Qiandao lake (PR of China). Adv. Struct. Eng. **11**, 439–454 (2008)
20. Reinertsen Olav Olsen Group: Feasibility study for crossing the Sognefjord. Submerged floating tunnel (2008)
21. Long, X., Ge, F., Wang, L., et al.: Effects of fundamental structure parameters on dynamic responses of submerged floating tunnel under hydrodynamic loads. Acta Mech. Sin. **25**, 335–344 (2009)
22. Wu, X., Ge, F., Hong, Y.S.: A review of recent studies on vortex-induced vibrations of long slender cylinders. J. Fluids Struct. **28**, 292–308 (2012)
23. Xu, Y., Guo, W.: Effects of bridge motion and crosswind on ride comfort of road vehicles. J. Wind Eng. Ind. Aerodyn. **92**, 641–662 (2004)
24. Huang, G., Wu, Y., Hong, Y.S.: Transportation of crossing waterways via Archimedes Bridge. Ship Build China **43** (supplement), 13–18 (2002)
25. Morison, J., O'Brien, M., Johnson, J., et al.: The force exerted by surface waves on piles. J. Petrol. Technol. Am. Inst. Min. Eng. **189**, 149–154 (1950)
26. Chakrabarti, S.K.: Hydrodynamics of Offshore Structures. WIT Press, Southampton (1987)
27. Chowdhury, I., Dasgupta, S.P.: Computation of Rayleigh damping coefficients for large systems. Electron. J. Geotech. Eng. 8: Bundle 8C (2003)
28. Det Norske Veritas: Recommended Practice DNV-RP-F105. Free spanning pipelines (2006)
29. Susumu, M., Akihide, T., Yuzo, M., et al.: Experimental study on characteristics of submerged floating tunnels under regular waves. In: Proceeding 3rd Symposium on Strait Crossings, Alesund, 667–674 (1994)
30. Clough, R.W., Penzien, J.: Dynamics of Structures. Mc Graw-hill, Inc, New York (1975)
31. Long, X.: Dynamic response of submerged floating tunnels with different buoyancy–weight ratios under wave and current loads: MS Dissertation. Institute of Mechanics, Graduate University of Chinese Academy of Sciences, Beijing, China (2008)
32. Wu, Y.S., Yang, Y.B.: Steady-state response and riding comfort of trains moving over a series of simply supported bridges. Eng. Struct. **25**, 251–265 (2003)
33. Hui, L., Li, Q., Hong, Y.S., et al.: Emergency escape devices of Archimedes Bridge, Patent No. CN 200510105226. China (2008)
34. Dong, M.S., Miao, G.P., Yong, L.C., et al.: Effect of escape device for submerged floating tunnel (SFT) on hydrodynamic loads applied to SFT. J Hydrodyn. **24**, 609–616 (2008)
35. Tariverdilo, S., Mirzapour, J., Shahmardani, M., et al.: Vibration of submerged floating tunnels due to moving loads. Appl. Math. Model. **35**, 5413–5425 (2011)
36. Jakobsen, B.: Design of the submerged floating tunnel operating under various conditions. ISAB **4**, 71–79 (2010)
37. Ge, F., Wang, L., Long, X., et al.: Design of submerged floating tunnel with adjustable buoyancy. Patent No. CN200810223702.0. China (2009)